Electromigration Induced Evolution of Voids in Current Crowding Areas of Interconnects

H. Ceric and S. Selberherr
Institute for Microelectronics, TU Vienna, Gusshausstrasse 27-29/E360, A-1040 Vienna
Phone: +43-1-58801/36032, Fax: +43-1-58801/36099 Email: Ceric@iue.tuwien.ac.at

1. Introduction

One of the most important issues in the reliability study of integrated circuits interconnect lines is electromigration. This phenomena results in the formation and growth of voids in metal interconnect which can cause significant fluctuations in interconnect resistance and in the extreme case sever the interconnect line. The electromigration failure occurs, according to different failure criteria by a resistance change of 10 to 20 %.

To accurately simulate interconnect resistance change due to electromigration, tracking the void shape and position is necessary. Simulations of void evolution in linear interconnect began with sharp interface models which showed the insufficiency of sharp interface models [1, 2]. Later, prompted by the complexity of void surface diffuse interface models were introduced [3]. An alternative diffuse interface model based on the double obstacle potential was proposed in [4]. However, all these methods require structured underlying meshes and were applied to simple rectangular interconnect geometries. To reach higher mesh adaptability and appropriate refinement quality for the finite element scheme solving diffuse interface model we used a version of recursive local mesh refinement algorithm introduced in [5].

2. Applied Diffuse Interface Model

We assumed unpassivated monocrystal isotropic interconnects where stress phenomena can be neglected. An interconnect is idealised as two-dimensional electrically conducting via which contains initially circular void. For simplicity we also neglect the effects of grain boundaries and lattice diffusion.

In such case there are two main forces which influence the shape of the evolving void interface: the chemical potential gradient and electron wind. The first force causes self-diffusion of metal atoms on the void interface and tends to minimize energy which results in circular voids shapes. The electron wind force produces asymmetry in the void shape depending on electrical field gradients. In the diffuse interface models, void and metal area presented through the order parameter ϕ which takes values $+1$ in the metal area, -1 in the void area and $-1<\phi<+1$ in the void-metal interface area. The model equations for the void evolving in an unpassivated interconnect line are for the order parameter ϕ [4],

$$\frac{\partial\phi}{\partial t}=\frac{2D_s}{\varepsilon\pi}\nabla\cdot\left(\nabla\mu-|e|Z^*\nabla V\right) \tag{1}$$

$$\mu=\frac{4\Omega\gamma_s}{\varepsilon\pi}\left(f'(\phi)-\varepsilon^2\Delta\phi\right) \tag{2}$$

and for the electrical field

$$\nabla\cdot\left(\sigma(\phi)\nabla V\right)=0 \tag{3}$$

Where D_s is the surface diffusivity, μ is the chemical potential, Z^* is the effective valence, e is the charge of the electron, γ_s is the surface energy, Ω is the volume of the atom, $f(\phi)$ is the double obstacle potential as defined in [4], ε is a parameter controlling the void-metal interface width and V is the electrical potential.

The electrical conductivity was taken to vary linearly from the metal $(\sigma=\sigma_{metal})$ to the void area $(\sigma=0)$ by setting $(\sigma=\sigma_{metal}(1+\phi)/2)$.

The equations (1) and (3) are solved on the 2D polygonal interconnect area T.

3. Numerical Implementation

3.1. Finite Element Scheme

Let be T_h a triangulation of the area T, and V_h finite element space of piecewise linear functions defined on T_h. We call T_h *basic triangulation* of area T. For $\varphi,\xi\in V_h$ an inner product on T is defined by $(\varphi,\xi)=\int_T\varphi\xi\,dxdy$.

As results of the constraints imposed on order parameter ϕ in equations (1) by the double obstacle potential $f(\phi)$, the weak formulation of the problem has the form of the variational inequality [11]

$$\varepsilon\frac{\pi}{2}\left(\frac{\partial\phi}{\partial t},\chi\right)+D_s(\nabla\mu,\nabla\chi)=0 \tag{4}$$

$$\frac{4\Omega\gamma_s\varepsilon}{\pi}(\nabla\phi,\nabla\chi-\nabla\phi)+\frac{4\Omega\gamma_s}{\varepsilon\pi}(\phi,\chi-\phi)-|e|Z^*V\geq(\mu,\chi-\phi) \tag{5}$$

where $\chi\in V_h$ and $|\chi|\leq 1$.

The numerical solution to the above variational inequality is computed using an iterative method known as projected SOR scheme [6].

An iteration for evaluating (ϕ^n,μ^n) consists of two steps:

Step 1.
For the k^{th} iteration of n^{th} time step linear system of equations has to be solved:

$$\varepsilon \frac{\pi}{2} M_{ii}\phi_i^{n,k} + \Delta t D_s K_{ii}\mu^{n,k} = \alpha_i \quad (6)$$

$$M_{ii}\mu^{n,k} - \frac{4\Omega\gamma_s}{\pi}\left(\frac{1}{\varepsilon}M_{ii} + \varepsilon K_{ii}\right)\phi^{n,k} = \beta_i, \quad (7)$$

where

$$\alpha_i = \varepsilon \frac{\pi}{2} M_{ii}\phi_i^{n-1} - \Delta t D_s \sum_{i\neq j} K_{ij}\mu_j^{n,k-1} \quad (8)$$

$$\beta_i = \frac{4\Omega\gamma_s\varepsilon}{\pi}\sum_{i\neq j} K_{ij}\phi_j^{n,k-1} - |e|Z^* M_{ii}V_i^{n-1} \quad (9)$$

for each $i = 1, N$ of nodal values (ϕ_i^n, μ_i^n) of the triangulation T_h. $[M]_{ij}$ and $[K]_{ij}$ are the lumped mass and stiffness matrix, respectively.

Step 2.
All nodal values of $\{\phi\}_{i=0}^{N-1}$ are projected on $[-1,+1]$ by a function

$$\rho(x) = \max(-1, \min(1, x)). \quad (10)$$

For solving of equation (3) a usual finite element scheme is applied [7].
As we will see in the next section, in order to reach appropriate accuracy, schemas for the finite element solving of the equations (1) and (3) require sequential mesh adaptation in each time step.
Let us denote $\Phi(\Lambda_h(t_n), t_n) = \{\phi_i\}_{i=0}^{N-1}$ the node value distribution of order parameter ϕ for the time step t_n on the mesh $\Lambda_h(t_n)$. The time dependent schema (20) can be represented symbolically as an operator H:

$$H \;:\; \Phi(\Lambda_h(t_n), t_n) \to \Phi(\Lambda_h(t_n), t_{n+1}) \quad (11)$$

For the mesh transformation we used a general adaptive algorithm Ψ with flexible refinement-coarsening pattern which transforms under certain defined condition $COND$ mesh $\Lambda_h(t_n)$ into mesh $\Lambda_h(t_{n+1})$ in the next time step.

$$\Psi(\Lambda_h(t_n), COND) = \Lambda_h(t_{n+1}) \quad (12)$$

The details of this adaptive algorithm will be described in a separate publication [8].

3.2. Dynamic Mesh Adaptation

The parameter ε in the equation (1) and (2) must be chosen sufficiently small to ensure that the diffuse interface model produces an adequate approximation of the void-metal interface shape and position. Evolving diffuse interface defined by equation (1) takes values between -1 and $+1$ in the inner of the thin interfacial region of width $\varepsilon\pi$. The mesh has to have enough triangle elements over the width of interfacial region to ensure smoothness of order parameter profile. The finer mesh region has also to be attached locally to the void-metal interface dynamically following the position of the interface and in order to avoid covering of larger portions of simulation area with a computer resources demanding fine mesh. Outside the interfacial area the basic mesh T_h should be sufficiently fine for the accurate evaluation of a electrical potential and order parameter.

3.2.1 Setting of the initial order parameter profile and initial mesh refinement $\Lambda_h(0)$

Initial order parameter profile depends on the initial shape of the void $\Gamma(0)$ and can be expressed as

$$\phi(x, y, t) = \begin{cases} 1 & if \quad d > \frac{\varepsilon\pi}{2} \\ \sin(\frac{d}{\varepsilon}) & if \quad |d| \le \frac{\varepsilon\pi}{2} \\ -1 & if \quad d < -\frac{\varepsilon\pi}{2} \end{cases} \quad (13)$$

Where $d = dist(P(x, y), \Gamma(0))$ is the signed normal distance of the point $P(x, y)$ from the initial interface $\Gamma(0)$. In order to enable sufficient resolution of this initial profile, the basic mesh T_h should be transformed into mesh $\Lambda_h(0)$ with respect to following criterion:
Initial mesh refinement criterion ($IMRC$) for the circular void with centre O and radius r is:

$$\forall\, K \in T_h \quad if\ |dist(C_K, O) - r| \le \frac{\varepsilon\pi}{2}\ than\ h_K < \frac{\varepsilon\pi}{n}$$

n is the chosen number of mesh elements across the void-metal interface width, h_K is the longest vertices of the triangle K and C_K its centre of gravity.
Now an adaptive algorithm Ψ transforms initial mesh T_h according to $IMRC$.

$$\Psi(T_h, IMRC) = \Lambda_h(0) \quad (14)$$

This means that each element of T_h is recursive adapted by algorithm Ψ until $IMRC$ is satisfied.
The initial order parameter distribution (6) is set on mesh $\Lambda_h(0)$ and has the symbolically the form:

$$\Phi(\Lambda_h(0), 0) \quad (15)$$

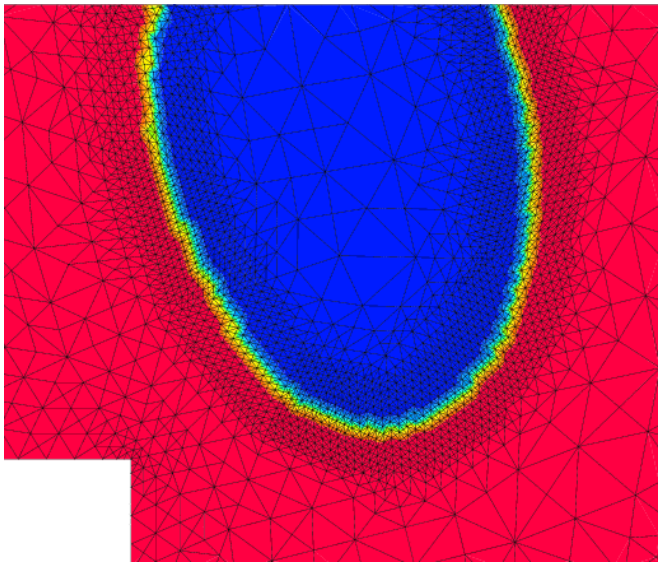

Fig. 1: Refined mesh around the void

3.2.2 Maintaining the mesh during the simulation

After an order parameter was evaluated on the $\Lambda_h(t_{n-1})$ a mesh needs to be readapted according to the new void-metal interface position.

Therefore it is necessary to extract all elements which are cut by void-metal interface in mesh $\Lambda_h(t_{n-1})$. The following condition is used: Let us take a triangle element $K \in \Lambda_h(t_{n-1})$ and denote its vertices as P_0, P_1, P_2. The triangle K belongs to the interfacial elements if for the values of order parameter ϕ at the triangle's vertices holds $\phi(P_0)\phi(P_1) < 0$ or $\phi(P_1)\phi(P_2) < 0$. We assume that an interface intersects each edge of the element only once (Fig. 1).

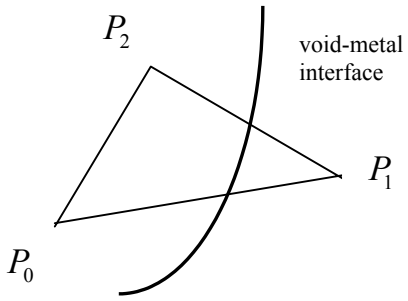

Fig. 1: Interface cutting chain element

The set of all interfacial elements at time t_{n-1} is denoted as $E(t_{n-1})$. The centres of gravity of each triangle from the $E(t_{n-1})$ build the interface point list $L(t_{n-1})$. The distance of the arbitrary point Q from $L(t_{n-1})$ is defined as

$$dist(Q, L(t_{n-1})) = \min_{P \in L(t_{n-1})} dist(Q, P). \qquad (16)$$

Thus we can define *the transitional mesh refinement criterion TMRC*

$$\forall\, K \in T_h \quad if\ dist(C_K, L(t_{n-1})) \le \frac{\varepsilon\pi}{2}\ than\ h_K < \frac{\varepsilon\pi}{n}$$

And the mesh adapting for the next time step evaluation of parameter ϕ can be expressed as

$$\Psi(\Lambda_h(t_{n-1}), TMRC) = \Lambda_h(t_n). \qquad (17)$$

TMRC ensures fine mesh resolution of the belt area of width $\varepsilon\pi/2$ around the newly evaluated void-metal interface with n elements across it.

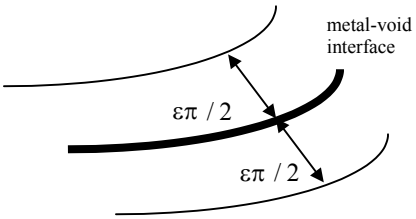

Fig. 2: Fine grid area around void-metal interface.

3.3. Solving Procedure

Based on the steps described in the sections above the complete solving procedure is represented by the diagram in Fig. 3.

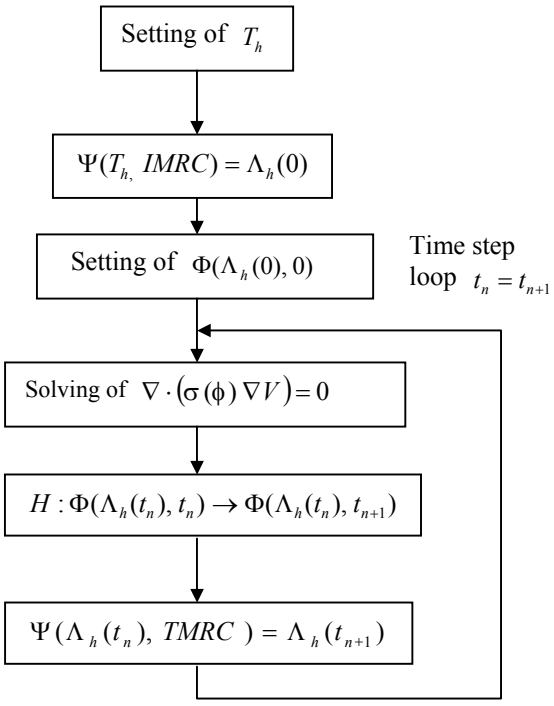

Fig. 3: Solving procedure

The maximal time step $\Delta t = t_{n+1} - t_n$ is chosen to ensure that the simulated void-interface does not overrun the belt area of the fine mesh.

4. Results and Discussion

We consider a two-dimensional, stress free, electrical conducting interconnect via. A constant voltage is prescribed at points A and B (Fig. 4.) of the structure. Because of geometrical reasons there is current crowding in the adjacencies of the corners C and D. The analytical solution of the equation (3) has in these points actually a singularity [7].

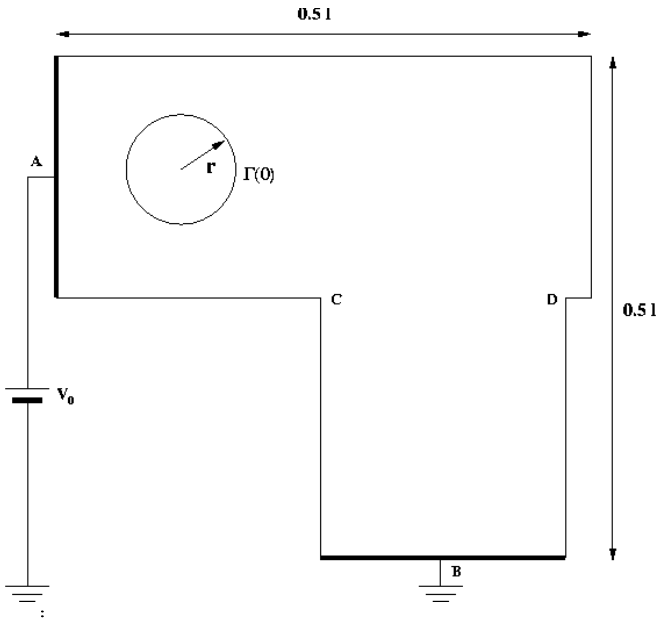

Fig. 4: Interconnect via with initial void

High electrical field gradients in the area around the corner points increase overall error of finite element schema for the equation (3) which is overcome by applying an additional refinement of the basic mesh T_h according to the local value of the electrical field gradient.

In our simulations void evolving through linear part of the interconnect geometry exhibits similar shape changes as observed in the earlier diffuse interface [3,4] and sharp interface models [1,2]. There is also no significant fluctuations of the resistance during this period of interconnect evolution. The situation changes when the void evolves in the proximity of the interconnect corner. Due to current crowding in this area (Fig. 5.) the influence of the electromigration force on the material transport on the void surface is more pronounced than the chemical potential gradient and this unbalance leads to higher asymmetry in the void shape then observed in the linear part of interconnect.

Our simulations have shown that even in this case voids follow the electrical current direction (Fig. 4.), but undergo more extensive shape changes than in the linear part of the interconnect.

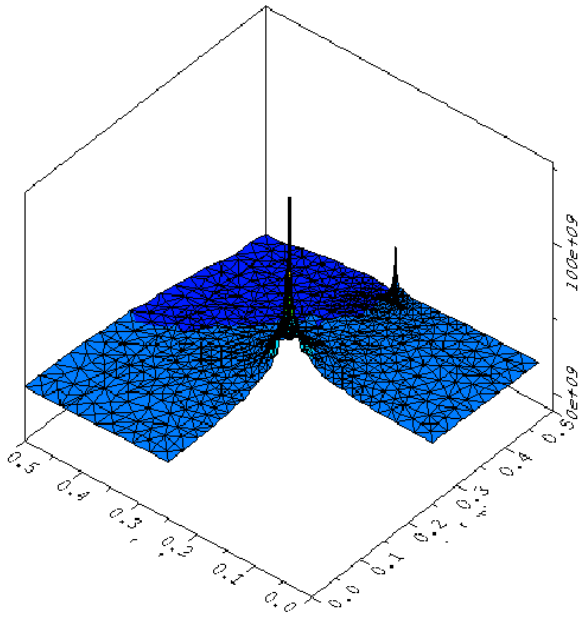

Fig. 5: Qualitative profile of the current density (in A/m^2) at the corners of interconnect

This shape change and the position of void at the interconnect corner causes characteristical profile of the resistance change which shows a lowering of the electromigration damage influence on the interconnect resistance for the time duration depending on the initial void size (Fig. 4.).

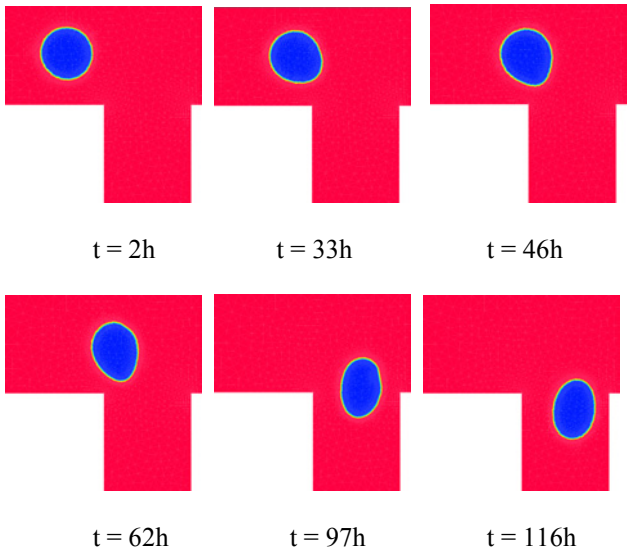

Fig. 4: Void evolving through interconnect in the electric current direction

It was also observed, that independent of the initial void size, voids retains it's stability and do not transform in slit or wedge like formations which have been shown to be a main cause for the complete interconnect failure [9, 10].

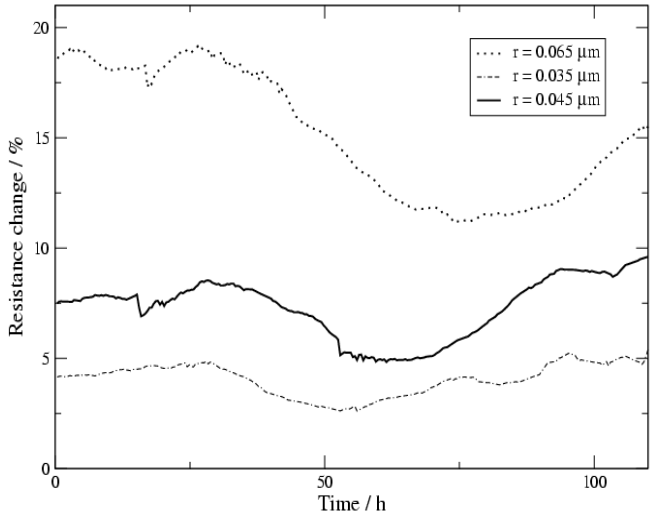

Fig. 4: Time dependent resistance change during void evolution for the different initial void radius r

The dynamic of the evolving void-metal interface simulated with a presented numerical schema comply with the mass conservation law, the void area (where $\phi = -1$) remains approximately the same during the whole simulations. Infect notable discrepancies appear only if the relatively huge factor ε has been chosen. As scaling length we took $l = 10^{-5}\,m$ and for initial void radius $r_0 = 0.035l$, $r_1 = 0.045l$, and $r_1 = 0.065l$ already with $\varepsilon = 0.003l$ good approximations are achieved. The number of elements on the cross section of the void-metal interface was chosen between 6 and 10.

The time step is fitted at the simulations begin taking into account inverse proportionality of the speed of evolving void-metal interface to the initial void radius [1]. Assuming the linear dependence of the void-metal interface speed of the applied voltage V_0 (Fig. 4.) during the time step Δt we get an approximation

$$\Delta t = \frac{\varepsilon \pi r l}{2 D_s |e| Z^* V_0} \tag{18}$$

Appropriate choice of the time step ensures that the evolving void-metal interface will stay inside the fine mesh belt during the simulation.

5. Conclusion

A governing diffuse interface equation for the order parameter coupled with the Laplace equation for the electrical field is solved using the finite element schema suited to dynamically adapted mesh. The mesh is maintained by an refinement-coarsening algorithm controlled by position, curvature and width of the simulated void-metal interface which distributes the mesh density in such a way that it allows an efficient simulation of evolving voids through large portions of complex interconnect geometry.

Due to high electrical current gradients in the proximity of the interconnect corners and overall asymmetry of the electrical field, voids exhibit specific faceting which was not observed in the case of the linear interconnect geometries. The presented method is well suited for long time prediction of resistance change due to electromigration during the interconnect life time. The applied diffuse interface model extends readily to incorporate the additional physical such as that of anisotropy, temperature variations and bulk and grain boundary diffusion.

References

[1] D. R. Fridline and A. F. Bower, "Influence of anisotropic surface diffusivity on electromigration induced void migration and evolution", *J. Appl. Phys., Vol. 85, no. 6, pp. 3168 – 3174, 1999*.

[2] M. R. Gungor and D. Maroudas, "Theoretical analysis of electromigration-induced failure of metallic thin films due to transgranular void propagation," *J. Appl. Phys., Vol. 85, no. 4, pp. 2233 – 2246, 1999*.

[3] R. B. M. Mahadevan, "Phase field model of surface electromigration in single crystal metal thin films," *Physica D, vol. 126, pp. 201-213, 1999.*

[4] D. N. Bhate, A. Kummar and A. F. Bower, "Diffuse interface model for electromigration and stress voiding ," *J. Appl. Phys., Vol. 87, no. 4, pp. 1712 – 1721, 2000*.

[5] I. Kossacky, "A recursive approach to local mesh refinement in two and three dimensions," *J. Comput. Appl. Math.,* vol. 55, pp. 275-288, 1994.

[6] C. Elliot and J. Ockendon, *Weak and Variational Methods for Moving Boundary Problems.* (Pitman Publishing Inc., Boston, 1981).

[7] R. Sabelka, *Dreidimensionale Finite Elemente Simulation von Verdrahtungsstrukturen auf Integrierten Schaltung.* Ph.D. Thesis, Technische Universität Wien, Institut für Mikroelektronik, Austria (2001).

[8] H. Ceric and S. Selberherr, "An adaptive grid approach for the simulation of electromigration induced void migration," to be published.

[9] E. Arzt, O. Kraft, W. D. Nix and J. E. Sanchez, Jr. „Electromigration failure by shape change of voids in bamboo lines," *J. Appl. Phys., Vol. 76, no. 3, pp. 1563-1571, 1994.*

[10] O. Kraft and E. Arzt, "Electromigration mechanism in conductor lines: void shape changes and slit-like failure," *Acta Mater., Vol. 45, no. 4, pp. 1599-1611, 1997.*

[11] J. F. Blowey and C. M. Elliot, "The Cahn-Hilliard gradient theory with non smooth free energy Part I: Mathematical analysis," *European Journal of Applied Mathematics, Vol. 2, pp. 233-279, 1991.*

Acknowledgements

This research project is supported by the European Community MULSIC project.